A family of γ-like calcium channel subunits

Norbert Klugbauer*, Shuiping Dai, Verena Specht, Lubica Lacinová[1], Elsé Marais, Georg Bohn, Franz Hofmann

Institut für Pharmakologie und Toxikologie der Technischen Universität München, Biedersteiner Str. 29, 80802 Munich, Germany

Received 6 December 1999; received in revised form 23 February 2000

Edited by Maurice Montal

Abstract The γ subunit was initially identified as an auxiliary subunit of the skeletal muscle calcium channel complex. Evidence for the existence of further γ subunits arose following the characterization of a genetic defect that induces epileptic seizures in stargazer mice. We present here the first account of a family of at least five putative γ subunits that are predominantly expressed in brain. The γ-2 and γ-4 subunits shift the steady-state inactivation curve to more hyperpolarized potentials upon coexpression with the P/Q type α_{1A} subunit. The coexpression of the γ-5 subunit accelerates the time course of current activation and inactivation of the α_{1G} T-type calcium channel.

© 2000 Federation of European Biochemical Societies.

Key words: Calcium channel; Gamma subunit; Voltage gated; Molecular diversity; Electrophysiology

1. Introduction

The purified skeletal muscle calcium channel complex consists of four subunits, the α_{1S}, β1a, $\alpha_2\delta$-1 and the γ subunit (for a review see [1]). Whereas different classes of the pore forming α_1 subunit and various auxiliary β and $\alpha_2\delta$ subunits have been identified in many other tissues, the γ subunit was for a long time thought to be unique to skeletal muscle. This subunit was originally purified from rabbit skeletal muscle and its cDNA sequence determined [2,3]. The genomic organization of the human and murine γ subunit have been determined and linkage mapping localized the γ-gene to human chromosome 17q24 [4–6]. Structurally the γ subunit contains four putative transmembrane segments separating intracellularly located N- and C-termini [2,3].

Coexpression studies revealed a modulatory function of the γ subunit on the L-type calcium channel; these include changes in peak current and in the activation and inactivation kinetics [7–9]. Reconstitution of the high affinity dihydropyridine binding activity of the skeletal muscle calcium channel requires the coexpression of γ together with α_{1S}, β and $\alpha_2\delta$-1 subunits [10].

Attempts to identify further γ subunits in tissues other than skeletal muscle by standard molecular biological techniques failed [9]. However, a second γ subunit was recently identified when a form of epilepsy in mice was found to be due to a defect in a γ subunit gene [11]. Mice with a disruption in this gene suffer from spike-wave seizures characteristic of absence epilepsy and are described as having a stargazer phenotype. A small shift in the steady-state inactivation curve towards hyperpolarized potentials was found upon coexpression of the calcium channel subunits α_{1A}, β1a, $\alpha_2\delta$-1 and γ-2. The defect of the γ-2 subunit probably caused a significant reduction in channel availability at typical neuronal resting potentials.

The existence of further γ subunits in brain could differentially modulate the availability of other neuronal calcium channels and thereby contribute to the diversity of high-voltage gated calcium channels. It is also possible that neuronal γ subunits could interact with the newly described T-type calcium channel subunits, three of which have been identified [12–15]. Since there are no marked modulatory effects of auxiliary $\alpha_2\delta$-1 or $\alpha_2\delta$-3 subunits on T-type channels [16,17] and due to a lack of the consensus motif for a β subunit interaction site (AID) in T-type calcium channel α_1 subunits, a possible interaction between the T-type α_{1G} and γ subunits was investigated.

2. Materials and methods

2.1. Molecular cloning

The basis of our cloning strategy was a detailed EST database search with γ-1 and γ-2 as probes using different search algorithms. Several partial sequences were obtained with different homologies to the previously known γ subunits. The following paragraphs summarize the cloning strategy for each γ subunit:

The partial EST hs905154 clone was initially identified and was used for the cloning of γ-3. During the progress of this work Black and Lennon [18] reported the human full-length sequence of this γ subunit. The mouse homologue of γ-3 described in this paper was PCR amplified from mouse brain cDNA using degenerate primers derived from the human γ-3 protein sequence.

The partial EST mm38636 clone was used to clone γ-4 from mouse brain. The full-length sequence was obtained by screening a cDNA library with EST mm38636 as a probe. Several independent clones were obtained and one of them was a full-length clone.

The basis for cloning of γ-5 were numerous overlapping EST clones (ai048969, aa881704, mm1155303, mmaa69349). Since these overlapping ESTs already contained the start and stop codons, a PCR approach was used to amplify the open reading frame as a single cDNA fragment from a mixed organ preparation from newborn mice. In addition, a mouse kidney cDNA library was screened with the PCR product. Sequencing of a library clone and of the PCR fragment confirmed their identity.

All cDNA clones and PCR fragments were sequenced on both strands with an automated ABI prism DNA sequencer (310 Genetic Analyzer).

The isolation of RNA and construction of the cDNA libraries as well as PCR techniques performed in this study are essentially the same as described in [19].

2.2. Northern blot and dot blot hybridization

Mouse multiple tissue Northern Blots and a human RNA Master blot were obtained from Clontech (Heidelberg, Germany) and hybrid-

*Corresponding author. Fax: (49)-89-4140 3261.
E-mail: klugbauer@ipt.med.tu-muenchen.de

[1] On leave from the Institute for Molecular Physiology and Genetics, Vlarska 5, 83334 Bratislava, Slovakia.

0014-5793/00/$20.00 © 2000 Federation of European Biochemical Societies. All rights reserved.
PII: S0014-5793(00)01306-5

ized according to the manufacturer's instructions. The following random-primed labelled fragments were used as probes: γ-3, nucleotides 131 to 853; γ-4, nucleotides 501–957; γ-5, nucleotides 131–508.

A 3 h prehybridization step was followed by an overnight hybridization with 5×10^6 cpm/ml of probe at 42°C. The final stringency wash performed was with 0.1×SSC, 0.1% SDS at 42°C.

2.3. Construction of a myc-fusion protein with γ-2 and expression in HEK293 cells

γ-2 cDNA was cloned in pcDNA3.1/Myc-His expression vector (Invitrogen) containing a *myc* epitope for the determination of the expression level in the eukaryotic host cells. The *myc* epitope is detectable using an anti-myc antibody.

9×10^6 HEK293 cells were transfected with α_{1A}, β_{1a}, $\alpha_2\delta$-1 (all the cDNAs were cloned in pcDNA3, see below) together with the recombinant protein γ-2 in pcDNA3.1/Myc-His using the calcium phosphate method. After transfection cells were harvested and resuspended in 1×PBS. The cell suspension was centrifuged and the pellet was resuspended in Buffer A (20 mM MOPS pH 7.4, 300 mM sucrose, 2 mM EDTA, 1 mM iodacetamide, 1 mM 1,10 phenanthroline, 0.1 mM phenylmethanesulfonyl fluoride, 1 μg/ml antipain, 1 μg/ml leupeptin and 1 mM benzamidine). Following homogenization, the extract was centrifuged for 10 min at $5000\times g$. The pellet was reextracted and centrifuged as before. The supernatants were combined and ultracentrifuged at $70\,000\times g$ for 35 min. The pellet was resuspended in buffer A and stored at −80°C.

The cellular localization of γ-2 was investigated using the anti-myc and a secondary Cy-3 labelled antibody (Dianova, Hamburg, Germany). The plasma membrane localization was established using a confocal laser scanning microscope.

2.4. Western blot analysis

Aliquots (about 2 and 4% of the membrane preparation) were loaded on a 10% SDS-polyacrylamide gel. The gel was blotted on a nitrocellulose membrane (Amersham) using an electroblotting apparatus (Bio-Rad). The primary anti-myc antibody (Invitrogen) was used at a 1:5000 dilution. Following washing, a secondary goat anti-mouse IgG-peroxidase conjugated antibody (Jackson Laboratories, West Grove, PA, USA) was applied. The proteins were detected using an ECL-system according to the manufacturer's instructions (Amersham).

2.5. In situ hybridization

Brains from adult mice were removed immediately following death by cervical dislocation and frozen in isopentane cooled to −40°C. The tissue was sectioned into 16 μm slices in a cryostat and thaw-mounted onto polylysine slides. Following vacuum drying for 30 min, the sections were fixed in 4% paraformaldehyde in PBS (20 min) and washed in 0.5×SSC (5 min). Sections were acetylated in 0.25% acetanhydride in 0.1 M triethanolamine, pH 8.0, for 10 min and washed twice with 2×SSC. The tissue was dehydrated through a series of ethanol solutions, from 50–100%. The slides were vacuum dried for 30 min and stored at −80°C until use.

The murine γ-2, γ-3 and γ-4 specific riboprobes were generated by in vitro transcription from a PCR template as follows. *Bam*HI and *Asp*718 restriction sites were added to forward and reverse primers, respectively, and probe template DNA amplified by PCR from the murine clones using primers specific for the variable C-terminal regions of γ-2 (nucleotides 820–947), γ-3 (nucleotides 748–912) and γ-4 (nucleotides 839–980), respectively. The insert was integrated by sticky-end ligation into a pUC19 derived plasmid containing T3 and T7 polymerase promoters. ^{35}S-UTP labelled sense and antisense riboprobes were produced using a standard T3, T7 polymerase in vitro transcription procedure [20]. Unincorporated nucleotide was removed with a Sephadex G50 column. The probes were applied at a specificity of 1×10^7cpm/ml in hybridization buffer (10 mM Tris, pH 8.0, 0.3 M NaCl, 1 mM EDTA, 1×Denhardt's, 10% dextran, 50% deionized formamide, 50 mM DTT, dithiothreitol and 0.5 μg/μl tRNA.

Messenger RNA in situ hybridization was performed on cryostat sections of mouse brain. Hybridization with the radiolabelled probe proceeded for 16 h at 55°C. The sections were washed in 2×SSC, 1 mM EDTA, 1 mM DTT and treated with 20μg/ml RNase in 0.2 M Tris–HCl pH 8.0, 1 M NaCl and 0.1 M EDTA to remove unbound probe. A high stringency wash of 0.1×SSC, 1 mM EDTA 1 mM DTT was done for 2 h at 60°C. The slides were dehydrated in ethanol and analyzed by autoradiography. Following autoradiography, the slides were coated with liquid film emulsion (Kodak NTB-2) and developed after 4–8 weeks. The slides were counterstained with toluidine blue and examined under dark- and bright-field illumination.

^{35}S-UTP was purchased from Amersham, the T3 and T7 polymerases from Stratagene Heidelberg, all enzymes used for ligation reactions were from New England Biolabs. The liquid film emulsion NTB-2 and Biomax, MR imaging film, developer and fixer were obtained from Kodak. All other reagents were of molecular biology grade.

2.6. Transfection of HEK293 cells

The full-length cDNAs of all subunits, i.e. α_{1C}, α_{1A}, α_{1G}, β1a, cardiac β2a [21], neuronal β2a [22], β3, $\alpha_2\delta$-1, $\alpha_2\delta$-2 and all γ cDNAs were cloned into the pcDNA3 vector (Invitrogen) or its derivative pcDNA3.1/Myc-His. HEK293 cells were transfected with various subunit combinations, each with the same amount of plasmid DNA. This was achieved by lipofection with Lipofectamine (Life Technologies) at a DNA mass ratio of 1:1 for expression of two, of 1:1:1 for three or 1:1:1:1 for four subunits.

2.7. Electrophysiological recordings

The whole-cell configuration of the patch clamp technique was employed as previously described [9]. Extracellular solutions used for experiments with high-voltage activated (HVA) channels were as follows: the α_{1A} channel: 110 mM NaCl, 20 mM tetraethylammonium chloride (TEA-Cl), 2 mM 4-aminopyridine, 10 mM $CaCl_2$ (or $BaCl_2$), 1 mM $MgCl_2$, 5 mM HEPES, 10 mM glucose, pH 7.4 (NaOH). The α_{1C} channel: 82 mM NaCl, 20 mM tetraethylammonium chloride (TEA-Cl), 2 mM 4-aminopyridine, 30 mM $BaCl_2$, 1 mM $MgCl_2$, 5 mM HEPES, 0.1 mM EGTA, 10 mM glucose, pH 7.4 (NaOH). For low-voltage activated (LVA) channels the extracellular solution contained: 110 mM *N*-methyl-D-glucamine, 20 mM $CaCl_2$, 5 mM CsCl, 1 mM $MgCl_2$, 10 mM HEPES, 10 mM glucose, pH 7.4 (HCl). The pipette solution for HVA channels contained: 120 mM CsCl, 10 mM TEA-Cl, 10 mM EGTA, 0.5 mM GTP, MgATP 3, HEPES 5, pH 7.4 (CsOH). For LVA channels the intracellular solution contained: 102 mM CsCl, 5 mM MgATP, 5 mM $NaCl_2$, 10 mM $TEACl_2$, 10 mM EGTA,10 mM HEPES, pH 7.4 (CsOH). Borosillicate glass pipettes had an input resistance between 1.5 and 3 MΩ. Series resistance was compensated up to 60%. Data were leak subtracted using a P/4 protocol. All experiments were carried out at room temperature (20–24°C). Whole-cell currents were recorded using an EPC-7 or EPC-9 amplifier and analyzed using the pCLAMP software from Axon Instruments and software from HEKA Electronic (Lambrecht, Germany). Curve fitting and statistical analysis were carried out using the Origin software (Microcal, Northampton, MA, USA). Data are given as mean ± S.E.M., statistical comparisons were performed using unpaired Student's *t*-test, and the value of $P<0.05$ was considered to be statistically significant.

3. Results

3.1. Primary structures

A database search was performed using the protein sequences of γ-1 and γ-2 as probes for the identification of similar expressed sequence tags (ESTs). This search uncovered additional ESTs with varying degrees of homologies to these calcium channel subunits. Overlapping EST sequences belonging to one gene were used to construct full-length open reading frames. These sequences were verified by a PCR strategy using different mouse tissues as well as by screening cDNA libraries (for details see Section 2). According to the chronological order of identification and sequence homologies we suggest the following nomenclature. The skeletal γ subunit is only distantly related to all the other members (about 25% sequence similarity) and is named γ-1. Three γ subunits identified in mouse brain are much more closely related (about 60% and higher). This brain subfamily is designated as γ-2, γ-3, and γ-4. A fifth γ subunit is only distantly related and is named γ-5. The primary structures of all the subunits known so far

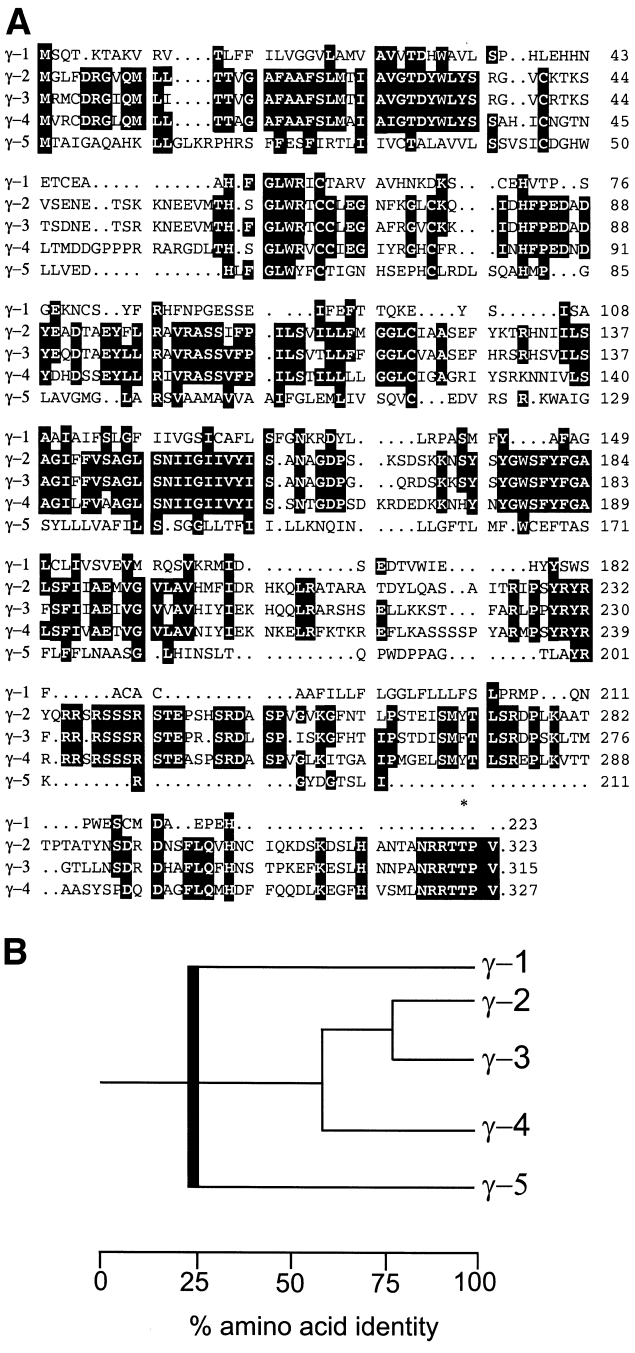

Fig. 1. Primary structure alignment of all known γ subunits (A) and their phylogenetic relations (B). A: γ-1 is a rat skeletal muscle specific γ subunit [9], γ-2 is a mouse γ subunit described in the stargazer mice by Letts et al. [11]. γ-3 to γ-5 have been identified in this study. White letters on black background indicate alignment positions with at least three identical residues. The asterisk indicates the C-terminal consensus site for cAMP/cGMP-dependent protein kinase phosphorylation site present in all neuronal γ subunits. The nucleotide sequences of the novel subunits are deposited under the accession numbers AJ272044, AJ272045 and AJ272046 in the EMBL database. B: Phylogenetic relations of the calcium channel γ subunit family. The thick bar at 25% amino acid sequence identity reflects the difficulty in reconstructing a correct phylogenetic tree with proteins with very low homology.
←

are presented in Fig. 1, together with a dendrogram showing the phylogenetic distances. The thick bar at approximately 25% sequence identity reflects the difficulty in constructing an alignment of proteins with very low homologies. γ-2 and γ-3 have 75.6% identical residues and both show about 60% identity with γ-4. The mouse γ-3 is 90.5% identical to the recently published human γ subunit sequence, indicating that the γ-3 presented in this study is the homologue of the human gene [18].

The γ-1 and γ-5 subunits are comparable in length (223 and 211 residues, respectively) and both have only a short C-terminal cytoplasmic region. The neuronal γ subunits are also similar in length and consist of 323, 315 and 327 residues for γ-2, γ-3 and γ-4, respectively. The difference in length between γ-1 and γ-5 and the brain subfamily is due to a long putative intracellular C-terminus. The nucleotide sequences upstream of the start ATG of all γ subunits are in agreement with that for the initiation of translation in eukaryotic host cells.

Hydrophobicity analyses were performed on all primary structures to confirm the presence of four putative transmembrane segments. In each case four hydrophobic segments could be identified (data not shown). Despite the low sequence homology between the γ-1 and γ-5 subunits, both have similar hydrophobicity profiles and have a highly conserved sequence motif (GLWxxC) and other common residues that are present in all five subunits. A common consensus site for cAMP/cGMP-dependent protein kinase phosphorylation is present in the intracellular C-terminus of all neuronal γ subunits (Fig. 1).

3.2. Tissue distribution

The tissue distribution of the novel putative γ subunits was analyzed by Northern blot and dot-blot hybridizations. Fig. 2 shows the results of a mouse multiple tissue Northern blot hybridization using γ-3 (Fig. 2A), γ-4 (Fig. 2B) and γ-5 (Fig. 2C) as probes. The length of the transcript for γ-3 is 2.4 kb and for γ-4 3.8 kb. The neuronal γ-2 subunit identified in stargazer mice is also only expressed in brain with an mRNA size of 6–7 kb and some additional smaller fragments [11]. γ-3 and γ-4 mRNAs were only detectable in mouse brain and even after a long time of autoradiography no signals were seen in other tissues. The γ-5 subunit is highly expressed in liver, kidney, heart, lung, skeletal muscle, and with a lower abundance in testes. The transcript size of γ-5 is 1.1 kb.

A dot-blot hybridization with human tissues using the same probes as for Northern analysis of γ-4 and γ-5 confirmed the above findings. This analysis indicates that the γ subunits are expressed in the same tissue specific manner in human as in mouse. The dot-blot hybridization also allows for the identification of γ specific transcripts in tissues not represented on the Northern blot. According to the dot-blot results, γ-4 is also expressed in fetal brain and at a very low level in the prostate (data not shown). The highest expression levels of γ-4 within brain were in caudate nucleus, putamen, thalamus, and frontal lobe. Expression analysis of γ-5 using the dot-blot hybridization was only confirmatory and did not reveal mRNA transcripts in other tissues.

3.3. In situ analysis

The mRNA expression of the novel brain γ subunits, γ-2 to γ-4, was studied in mouse brain sections (Fig. 3). The distri-

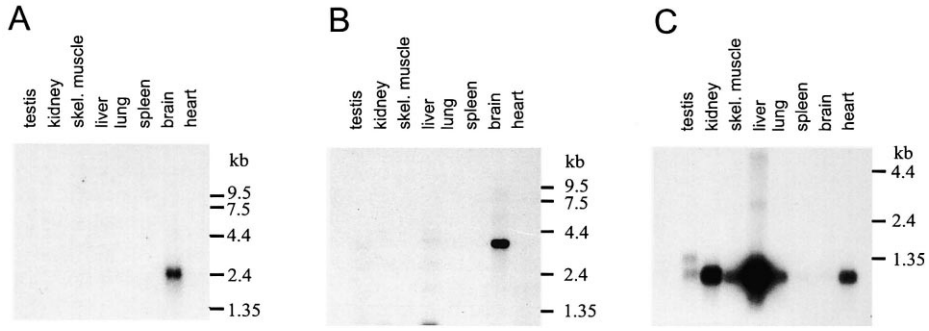

Fig. 2. Northern Blot hybridization of the γ-3 (A), γ-4 (B) and γ-5 (C) subunits. Each lane of the mouse multiple tissue blots contains about 2 μg of poly(A) RNA. Hybridization was performed according to the manufacturers instructions. The mRNA sizes are as follows: γ-3 2.4 kb, γ-4 3.8 kb and γ-5 1.1 kb.

bution of the γ subunits was found to differ considerably from each other. γ-2 was strongly detected in the cerebellum and moderately expressed in the hippocampus, cerebral cortex, thalamus and olfactory bulb (Fig. 3A; compare with [11]). γ-3 showed a strong expression in the hippocampus, the cerebral cortex and a moderate expression in the olfactory bulb and caudate putamen (Fig. 3B,C). γ-4 was found to be highly expressed in the caudate putamen, olfactory bulb, habenulae and to a lower level in the cerebellum and thalamus. (Fig. 3D–F). Examination of the tissue under higher magnification shows that the expression of γ-4 and γ-2 in the cerebellum originates predominantly from the Purkinje cell layer and not the granular cell layer.

3.4. Expression studies as myc fusion protein

Since the electrophysiological effects of the γ subunits upon coexpression with different α_1 subunits were very small (see below), the presence of the γ protein in the membranes of transfected HEK293 cells was validated by an immunocytochemical approach. The γ-2 cDNA full-length sequence was fused to the myc epitope at its C-terminus. Following transient transfection of the calcium channel subunits α_{1A}, β1a, $\alpha_2\delta$-1 and γ-2myc, membrane preparations were analyzed by Western blot (Fig. 4A). A 42 kDa protein was detected using an anti-myc antibody. The fusion protein of γ-2myc has a calculated molecular mass of 39 kDa. This difference is probably due to glycosylation of this subunit. These results are consistent with the observed 35 and 38 kDa proteins described by Letts and coworkers [11], which correspond to the deglycosylated and glycosylated forms of γ-2. Additionally the plasma membrane localization of γ-2 was established using confocal laser scanning microscopy (Fig. 4B)

3.5. Functional characterization

Functional characterization of the novel γ subunits was performed in coexpression studies with three different α_1 subunits of HVA and LVA calcium channels. Different subunit combinations were used for transient transfection of HEK293 cells. In a first series of experiments the same α_1, β and $\alpha_2\delta$ subunits were used as described by Letts and coworkers [11]. With the combination of α_{1A}, β1a, and $\alpha_2\delta$-1, the modulation of voltage-dependent activation and inactivation by γ subunits on I_{Ca} was investigated. Fig. 5A shows the conductance-voltage relations of I_{Ca} in the absence and presence of different

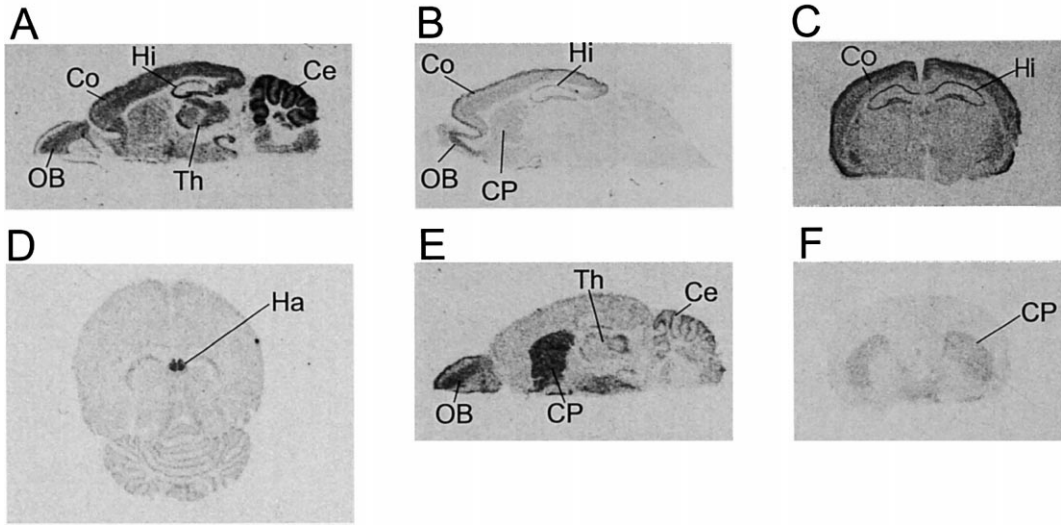

Fig. 3. Autoradiographs of γ-2 (A), γ-3 (B,C) and γ-4 (D–F) riboprobe hybridizations to mouse brain sections. γ-2 was strongly detected in the cerebellum and moderately in the hippocampus, cerebral cortex and olfactory bulb (compare with [11]). γ-3 mRNA was detected in the hippocampus, cortex, olfactory bulb and caudate putamen. γ-4 was found to be highly expressed in the caudate putamen, olfactory bulb, habenulae and at lower levels in the thalamus and cerebellum.

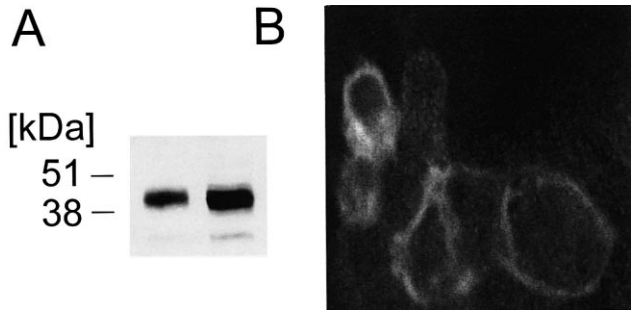

Fig. 4. Western blot analysis of the γ-2Myc-His fusion protein transiently expressed in HEK293 cells (A) and its plasma membrane localization (B). A: About 2% (left lane) and 4% (right lane) of the cell preparation (see Section 2) were run on a 10% SDS polyacrylamide gel, electroblotted to a nitrocellulose membrane and incubated with a myc-antibody. The size of the γ-2Myc-His fusion protein is about 42 kDa. The calculated molecular mass is 39 kDa, this difference presumably is caused by the glycosylation of the γ protein. B: Confocal laser scanning microscopy of the γ-2Myc-His fusion protein detected with an anti-myc and a secondary Cy-3 labelled antibody.

γ subunits. Only γ-2 showed a small but significant shift of the voltage-dependent activation to more positive potentials (Fig. 5 and Table 1).

As described by Letts et al. [11], γ-2 shifted the steady-state inactivation curve towards more hyperpolarized potentials (Fig. 5B and Table 1). This shift in the steady-state inactivation curve was also observed upon coexpression with γ-4, but not with γ-5. The γ-3 subunit was not further characterized in this study because of its close sequence similarity with γ-2, and the expection that they would behave similarly. Fig. 5C shows a comparison of the kinetics of inactivation of α_{1A} upon coexpression with different γ subunits. $\tau 1$ and $\tau 2$ were significantly reduced by the γ-2 and γ-4 subunits. In all experiments γ-5 had no significant effect on the modulation of voltage-dependent activation and inactivation of the α_{1A} calcium channel.

The above experiments were carried out with the skeletal muscle β1a subunit. In order to investigate the functional role of the β subunit and to use only subunits which have been cloned from brain, we repeated these experiments with the neuronal β2a (nβ2a) splice variant [22]. The same effect on the steady-state inactivation, that was seen with β1a could be observed when γ-2 was coexpressed with α_{1A}, β2a and $\alpha_2\delta$-1 (Fig. 6A and Table 1). However, the negative shift in the voltage-dependence of inactivation only occurred when Ca^{2+} was used as charge carrier. Using Ba^{2+} as charge carrier we observed a shift to more positive potentials (Fig. 6 and Table 1). In Fig. 6B the voltage dependency of the conductances are compared in the presence and absence of the γ-2 subunit either with Ca^{2+} or Ba^{2+} as charge carrier. The voltage dependent activation was shifted to hyperpolarized potentials when Ba^{2+} was used as charge carrier. The coexpression of the γ-2 subunit had no significant effect on activation when either Ca^{2+} or Ba^{2+} was used as charge carrier.

The interactions of the novel γ subunits were only analyzed with a member of the neuronal non-L-type calcium channels.

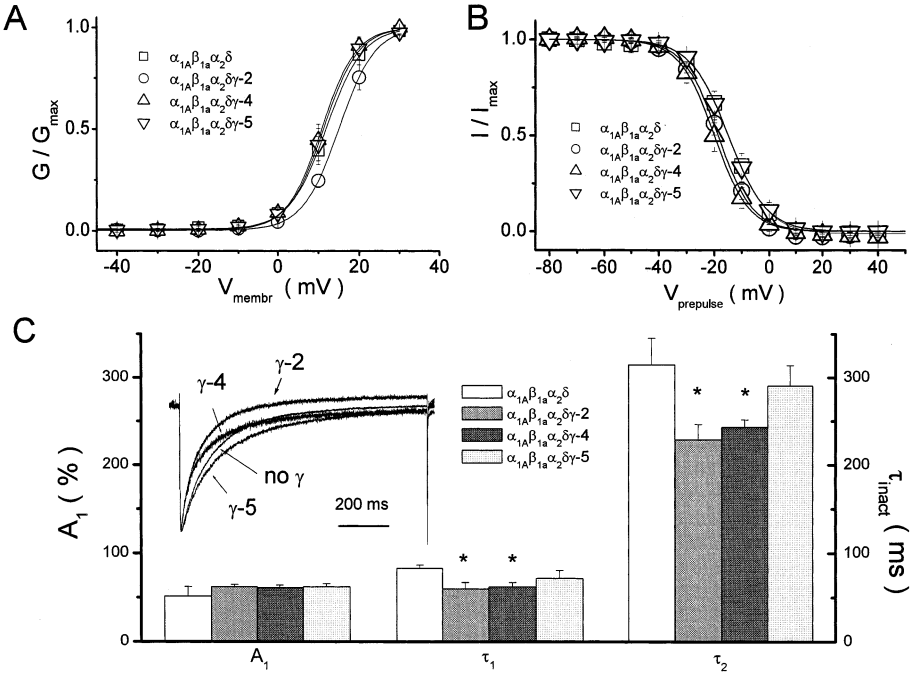

Fig. 5. Modulation of the voltage-dependent activation and inactivation of α_{1A} calcium channels by various γ subunits. The different subunit combinations are indicated in the insets. A: Conductance-voltage relation of I_{Ca} in the absence and presence of different γ subunits. The conductance (G) was calculated according to the equation $G(V) = I/(V - V_{rev})$ (see legend to Table 1). The data were averaged and fitted with the Boltzmann equation. B: Steady-state inactivation curves measured for I_{Ca} in the absence and presence of different γ subunits. The current was activated by a 100 ms long depolarizing pulse from a holding potential of −80 mV to +20 or +10 mV immediately after a 3 s long conditioning prepulse to voltages between −80 mV and +50 mV in 10 mV increments. The current amplitudes were normalized to the maximal amplitude. Solid lines represent Boltzmann fit. C: Comparison of the inactivation properties of the α_{1A} calcium channel upon coexpression with different γ subunits. The inset shows the time courses of I_{Ca} evoked by a 1 s long depolarizing pulse to +20 mV normalized to the same amplitude. I_{Ca} was best fitted with a sum of a two-exponential decay and are presented as columns. A_1 represents the percentage of the fast part of inactivation (τ_1). *: significant difference at $P < 0.05$.

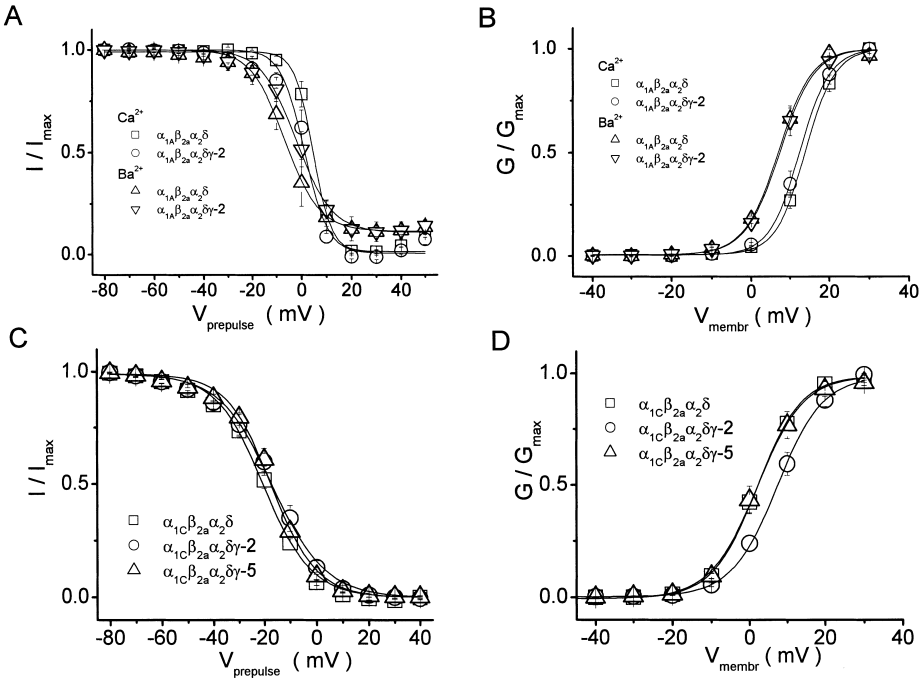

Fig. 6. Comparison of the steady-state inactivation curves and conductances of I_{Ca} and I_{Ba} through α_{1A}nβ2aα_2δ-1 or α_{1C}cβ2aα_2δ-1 calcium channels in the absence and presence of γ subunits. The different subunit combinations are indicated in the insets. A: Steady-state inactivation of I_{Ca} or I_{Ba} in HEK293 cells transfected with α_{1A}nβ2aα_2δ-1 in the absence or presence of the γ-2 subunit. 10 mM Ca^{2+} or Ba^{2+} were used as charge carrier. The same pulse protocol and analysis was employed as described in the legend to Fig. 5. B: Boltzmann fits of the voltage dependencies of the conductances as for the same subunit combination as in A. C: Steady-state inactivation of I_{Ba} in HEK293 cells transfected with α_{1C}cβ2aα_2δ-1 in the absence and presence of either the γ-2 or γ-5 subunit. The steady-state inactivation of I_{Ba} was evaluated by means of a 3 s long conditioning prepulse following a 200 ms test pulse from a holding potential of −80 mV. Solid lines represent Boltzmann fits. D: Boltzmann fits of the voltage dependencies of the conductances for the same subunit composition as in C.

We therefore compared the effects of the novel γ subunits with those of our previously published results on the L-type calcium channel α_{1C} [9]. Upon coexpression of γ-1 with α_{1C-a}, cardiac β2a (cβ2a) and α_2δ-1, the steady-state inactivation curve was shifted about 30 mV to more negative potentials and the current inactivation was accelerated. Using the newly identified subunits, γ-2 and γ-5, we performed coexpression studies with α_{1C-a}, cardiac β2a and α_2δ-1 with Ba^{2+} as charge carrier. Small but significant shifts of the voltage dependence of activation and inactivation were observed with γ-2, but not with the γ-5 subunit (Fig. 6C,D). These results suggest that there is also an interaction between the γ-2 subunit and the L-type calcium channel α_{1C}. Coexpression studies with γ-5 were also performed in the absence of α_2δ-1. The absence of this subunit did not uncover effects of γ-5 on the voltage dependence of activation or on the steady-state inactivation of the current through α_{1C} calcium channels. Although γ-5 is expressed in at least some of the tissues that also express

Table 1
The effects of different γ subunits on the activation and inactivation properties of calcium channels in various subunit combinations

Channel	Density (pA/pF)	Activation		*n*	Inactivation		*n*
		$V_{0.5\ activ.}$ (mV)	k_{activ}		$V_{0.5\ inact.}$ (mV)	k_{inact}	
α_{1A}β1aα_2δ (Ca^{2+})	34.8 ± 8.7	+11.9 ± 0.1	4.5 ± 0.1	8	−15.0 ± 0.3	6.9 ± 0.2	7
α_{1A}β1aα_2δγ-2 (Ca^{2+})	29.9 ± 3.4	+15.0 ± 0.1*	4.4 ± 0.1	9	−18.7 ± 0.4*	6.3 ± 0.4	9
α_{1A}β1aα_2δγ-4 (Ca^{2+})	35.9 ± 9.3	+10.8 ± 0.2	4.2 ± 0.2	8	−20.0 ± 0.3*	6.3 ± 0.3	6
α_{1A}β1aα_2δγ-5 (Ca^{2+})	36.0 ± 8.9	+11.3 ± 0.2	4.3 ± 0.2	9	−14.9 ± 0.2	6.9 ± 0.2	8
α_{1A}nβ2aα_2δ (Ca^{2+})	40.8 ± 2.7	+13.9 ± 0.2	3.8 ± 0.1	9	+4.6 ± 0.5	3.6 ± 0.3	8
α_{1A}nβ2aα_2δγ-2 (Ca^{2+})	42.9 ± 8.4	+12.4 ± 0.1	3.9 ± 0.1	10	+1.3 ± 0.8*	4.6 ± 0.7	8
α_{1A}nβ2aα_2δ (Ba^{2+})	45.9 ± 8.8	+6.9 ± 0.4	4.4 ± 0.2	8	−6.5 ± 0.5	6.9 ± 0.4	6
α_{1A}nβ2aα_2δγ-2 (Ba^{2+})	46.5 ± 6.2	+7.3 ± 0.3	4.5 ± 0.2	8	−1.9 ± 0.7*	7.0 ± 0.6	6
α_{1C}cβ2aα_2δ (Ba^{2+})	62.8 ± 7.0	+2.0 ± 0.4	5.9 ± 0.2	18	−19.8 ± 0.6	9.8 ± 0.6	16
α_{1C}cβ2aα_2δγ-2 (Ba^{2+})	45.1 ± 8.2	+7.3 ± 0.3*	6.1 ± 0.2	9	−16.5 ± 0.7*	11.2 ± 0.6	7
α_{1C}cβ2aα_2δγ-5 (Ba^{2+})	59.9 ± 9.7	+1.9 ± 0.4	6.2 ± 0.3	11	−17.2 ± 0.6	9.1 ± 0.5	8

HEK293 cells were transiently transfected with cDNA plasmids encoding channels with different combinations of α_{1A}, α_{1C}, β1a, β2a (brain or cardiac), α_2δ-1 and various γ subunits. For α_{1A} we used either β1a or the neuronal β2a and for α_{1C} we used the cardiac β2a splice variant. To analyze the voltage-dependent activation, the conductance (G) was calculated according to the equation $G(V) = I/(V - V_{rev})$, where I was the current, V was the test pulse potential and V_{rev} was the measured reversal potential. The data were averaged and fitted with the Boltzmann equation: $G(V) = G_{max}/\{1+\exp[(V - V_h)/k]\}$ (V_h is the potential of half the maximal activation and k is the slope). Steady-state inactivation was measured by a prepulse protocol. The average data were fitted with the Boltzmann equation as shown in Figs. 5 and 6. Data represent the mean ± S.E.M. The number of cells is indicated in parentheses. * Marks significant differences with $P < 0.05$.

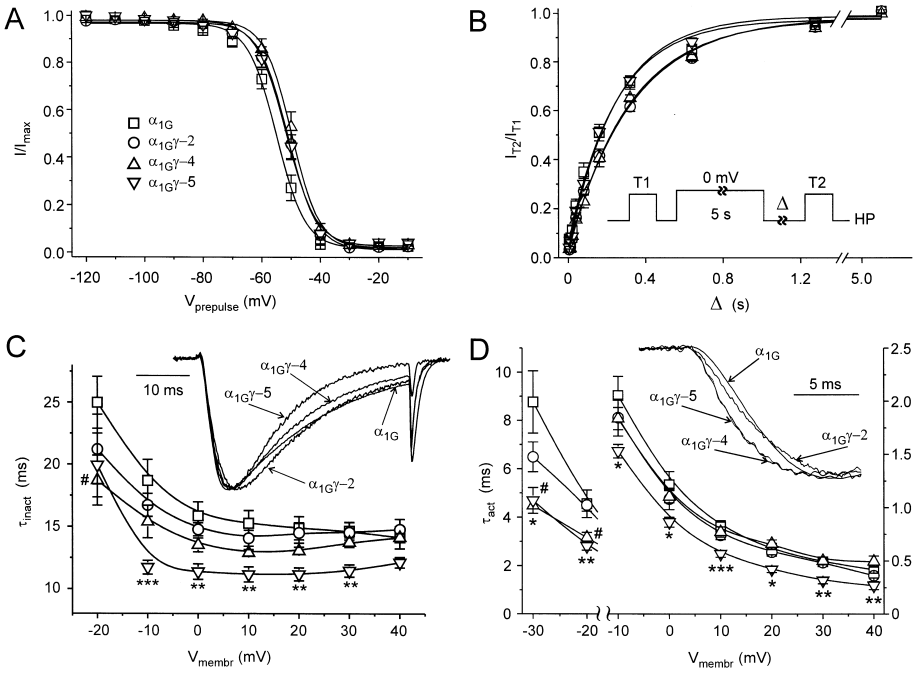

Fig. 7. Effects of the γ subunits on the voltage dependence of activation and inactivation of the α_{1G} channel. A: Steady-state inactivation curves were measured using the following protocol: transfected cells were held at −100 mV. 5 s long conditioning prepulses to voltages between −120 mV and −10 mV were followed by a 5 ms long return to −100 mV and by 40 ms long test pulses to the peak of the current–voltage relationship (−10 mV in most cases). The pulse sequence was repeated every 10 s. Amplitudes of test pulse currents were normalized to the maximal test pulse amplitude and averaged. Solid lines represent fits of averaged experimental data to the Boltzmann equation. (□), α_{1G} channel; (○), α_{1G}+γ-2 channel; (△) α_{1G}+γ-4 channel; (▽) α_{1G}+γ-5 channel. B: Recovery from voltage-dependent inactivation was measured using the voltage protocol shown in the inset. Briefly, current amplitude was tested by 40 ms long pulse to the peak of current–voltage relationship (T1). Channel was inactivated by a 5 s long pulse to 0 mV. After a variable recovery period Δ current amplitude was tested again by test pulse T2 identical to T1. Extent of recovery was evaluated as I_{T2}/I_{T1}. Same symbols as in A. C: Voltage dependence of time constants of current inactivation. The current was activated by depolarizing pulses from a holding potential (HP) of −100 mV to membrane voltages between −20 mV and +40 mV. Individual time courses were fitted to the Hodgkin–Huxley equation (m4h). The inset demonstrates the ascending phase of currents recorded during depolarization to −10 mV (peak of current–voltage relationship) normalized to the same amplitude. Symbols as in A. D: Voltage dependence of time constants of current activation obtained as described for C for membrane voltages between −30 mV and +40 mV. The same symbols as in A. The inset shows an example of current traces measured during a test pulse to −20 mV normalized to the same amplitude to facilitate comparison. Solid lines are connectors of experimental data. Please note different scales for depolarizations to −30 and −20 mV (left axis) and for depolarizations between −10 and +40 mV (right axis). # marks significant difference between α_{1G} channel and α_{1G}+γ-4 channel ($P<0.05$). *: Marks significant difference between α_{1G} channel and α_{1G}+γ-5 channel (*: $P<0.05$; **: $P<0.01$; ***: $P<0.001$).

α_{1C}, it does not seem to modulate this L-type calcium channel. For these reasons, we suggest that the γ-5 subunit may not be an auxiliary subunit of the high voltage gated calcium channel.

There is no typical β subunit interaction domain motif in T-type calcium channels and antisense strategies have shown no effects of β subunits on T-type current [23]. We therefore considered the possibility that the novel γ subunits are auxiliary subunits of the LVA T-type calcium channels and analyzed the effects of the γ-2, γ-4, and γ-5 subunits on the α_{1G}

Table 2
Effects of γ subunits on the voltage-dependent activation and inactivation of the α_{1G} T-type calcium channel

Channel	I (pA/pF)	Activation		Inactivation		
		$V_{0.5}$ (mV)	k	$V_{0.5}$ (mV)	k	τ (ms)
α_{1G}	62 ± 7 (25)	−24.9 ± 1.2 (12)	3.9 ± 0.3	−54.9 ± 1.2 (9)	4.3 ± 0.2	251 ± 24 (9)
α_{1G}γ-2	87 ± 13 (13)	−24.4 ± 1.6 (10)	3.8 ± 0.2	−51.4 ± 1.4 (10)	4.2 ± 0.2	336 ± 14** (8)
α_{1G}γ-4	79 ± 12 (14)	−23.9 ± 1.3 (10)	4.1 ± 0.2	−50.0 ± 1.4* (11)	3.9 ± 0.2	320 ± 17* (10)
α_{1G}γ-5	73 ± 9 (22)	−24.1 ± 1.0 (12)	3.9 ± 0.2	−51.7 ± 1.2 (11)	4.5 ± 0.2	248 ± 11 (9)
$\alpha_{1G}\alpha_2$δ-2	93 ± 15* (17)	−22.3 ± 0.8 (12)	4.1 ± 0.2	−50.4 ± 0.7** (11)	4.0 ± 0.2	279 ± 12 (10)
$\alpha_{1G}\alpha_2$δ-2γ-5	85 ± 12 (18)	−21.4 ± 1.1 (19)	4.2 ± 0.2	−49.3 ± 1.1** (11)	4.1 ± 0.3	296 ± 25

I represents averaged current densities for all tested channels. Activation was evaluated by fitting individual conductance–voltage relation calculated as described in the legend to Table 1 by the Boltzmann equation. Resulting $V_{0.5}$ and k values were averaged and are given in the third and fourth columns. Steady-state inactivation data were measured as described in the legend to Fig. 7 and were fitted by the Boltzmann equation. Resulting $V_{0.5}$ and k values for voltage dependent inactivation were averaged. The last column shows the time constant of recovery from voltage dependent inactivation measured as described in the legend to Fig. 7. Individual measurements were fitted to the exponential association curve and resulting τs were averaged. *: $P<0.05$ between α_{1G} and α_{1G}γ-4 channels; **: $P<0.01$ between α_{1G} and α_{1G}γ-2. Data are given as mean ± S.E.M. with the number of cells in brackets.

calcium channel with 20 mM Ca^{2+} as charge carrier. The current density was enhanced upon coexpression of each γ subunit, but this increase was not statistically significant (Table 2). The voltage dependence of current activation was unaffected. The steady-state inactivation curves were slightly shifted to more positive voltages (Table 2 and Fig. 7A), however, this shift was only significant for the γ-4 subunit. The speed of recovery from voltage-dependent inactivation was significantly slowed down by the γ-2 and γ-4 subunits, but not by the γ-5 subunit (Table 2 and Fig. 7B). The time course of current activation and inactivation during a depolarizing pulse was described by fitting individual records according to the Hodgkin–Huxley equation. The γ-5 subunit significantly accelerated both processes over the whole range of voltages. This effect indicates that γ-5 could be an auxiliary subunit of LVA calcium channels. In contrast, the γ-4 subunit had similar effects only at voltages above the threshold for current activation and the γ-2 subunit was without effect (Fig. 7C,D).

It is possible that an interaction of the γ-5 subunit with α_{1G} requires the presence of an additional auxiliary subunit. Due to the lack of a β subunit interaction domain in α_{1G}, potential candidates are the $\alpha_2\delta$ subunits. While $\alpha_2\delta$-1 and $\alpha_2\delta$-3 did not modulate the α_{1G} current [16], $\alpha_2\delta$-2 shifted significantly the voltage dependence of the steady-state inactivation of the channel (Table 2). Therefore we coexpressed α_{1G} together with $\alpha_2\delta$-2 and γ-5. However, the properties of the $\alpha_{1G}/\alpha_2\delta$-2/γ-5 channel were similar to the properties of the $\alpha_{1G}/\alpha_2\delta$-2 channel (Table 2).

4. Discussion

We present here the first account of the existence of a family of putative calcium channel γ subunits with at least five members. An amino acid alignment reveals that only the three neuronal γ subunits show a high degree of homology with each other. Furthermore the subunits of this subfamily are significantly longer at their C-terminal ends than the other γ subunits.

All neuronal γ subunits investigated so far shift the steady-state inactivation curve towards hyperpolarized potentials when coexpressed with α_{1A} in the presence of Ca^{2+} as charge carrier. As already suggested by Letts and coworkers [11] this shift may reduce the channel availability at a neuronal resting potential of −70 mV. Stargazin (γ-2) could inhibit presynaptic Ca^{2+} entry at nerve terminals, where P/Q-type calcium channels are abundant. The α_{1A} subunit has been shown to form P/Q-type calcium channels and alternative splicing of the α_{1A} subunit gene results in channels with distinct kinetic and pharmacological properties [24]. Clearly, the negative shift in the steady-state inactivation curve depends on the presence of Ca^{2+}. Using Ba^{2+} as charge carrier we found a small but significant shift to more positive potentials.

The in situ hybridization of γ-4 in mouse brain indicates a high expression in the caudate putamen and in the olfactory bulb. A comparison with the expression pattern of α_1 subunits reveals that α_{1A} and α_{1E} are the predominantly expressed HVA calcium channel subunits in these brain regions [20,25]. These observations further strengthen the physiological relevance of our coexpression experiments.

We further compared the effect of γ-2, as a representative of the neuronal γ subunits, and γ-5 as a more ubiquitously expressed subunit, with our previous results using the L-type calcium channel α_{1C} together with cardiac β2a and $\alpha_2\delta$-1 [9]. Upon coexpression of γ-1 with α_{1C-a}, cardiac β2a, $\alpha_2\delta$-1, the steady-state inactivation curve was shifted to negative potentials and the current inactivation was accelerated. These effects were essentially the same as observed by Singer et al. [7], who found that once present, the γ subunit dominates the inactivation process. However, none of the γ subunits investigated in this study showed this strong effect when coexpressed with α_{1C}. γ-2 even shifted the steady-state inactivation curve towards more positive potentials using Ba^{2+} as charge carrier. The physiological relevance of this observation is still unknown.

We also considered the possibility that the novel γ subunits are auxiliary subunits of T-type calcium channels. Coexpression with the T-type α_{1G} subunit revealed that the γ-2 and γ-4 subunits moderately increased the current density and slowed down the speed of recovery from voltage dependent inactivation. These relatively small effects are comparable with the effects of $\alpha_2\delta$ subunits on the T-type calcium channels [16,17] and may be the result of an improved targeting of the heterologously expressed calcium channel subunits. However, none of the auxiliary subunits had marked influences on the voltage dependence or kinetics of expressed α_{1G} currents. This could reflect the fact that the native subunit composition is still unknown or that the γ subunits interact with so far unidentified ion channels.

The Northern blot of γ-5 indicates a more ubiquitous expression pattern of this subunit, for example liver, heart, kidney, skeletal muscle and lung. T-type calcium channel α_1 subunits are also found in the liver and kidney (α_{1H} and α_{1I}) and in the heart (α_{1H} and α_{1G}). In order to test a potential association of the γ-5 subunit with a T-type calcium channel, we investigated the effects of the γ-5 subunit on α_{1G} in the presence and absence of the $\alpha_2\delta$-2 subunit. This $\alpha_2\delta$ subunit is expressed in heart and brain [19,26]. Expression of $\alpha_2\delta$-2 with α_{1G} increased the current density, accelerated the decay and shifted the steady-state inactivation of the current through α_{1G}. Coexpression of the γ-5 subunit together with α_{1G} and $\alpha_2\delta$-2 did not further increase the current density, and did not affect the other kinetic parameters. However, in the absence of the $\alpha_2\delta$-2 subunit, the γ-5 subunit accelerated the time course of current activation and inactivation of the T-type calcium channel. This interaction appears to be specific for T-type channels since the γ-5 subunit did not modulate the voltage dependence of activation and inactivation of the HVA α_{1A} and α_{1C} calcium channels. It is therefore conceivable that the γ-5 subunit interacts in vivo with T-type calcium channels.

In summary, we present here a family of γ subunits with at least five members which are expressed in a tissue specific manner. The neuronal γ-2, γ-3 and γ-4 subunits are expressed in different brain regions. The results of this and other studies [11,18] suggest, that γ-2, γ-3 and γ-4 could be associated with the α_{1A}, α_{1B} and α_{1E} channels. The in situ hybridizations from this and a previous study [25] suggest that γ-4 could be part of the α_{1E} calcium channel in the habenulae. Other brain regions express several α_1 and γ subunits. It is possible that γ-2 is preferentially part of the P/Q-type channel [11], whereas γ-3, γ-4 and γ-5 complex with other calcium channels or even with other membrane proteins not identified so far.

Acknowledgements: We thank Drs. S. Zimmer and V. Flockerzi (Homburg/Saar) for the cDNA plasmid of the α_{1A} calcium channel

subunit and Drs. N. Qin and L. Birnbaumer for the neuronal β2a subunit plasmid. We are grateful to Dr. H. Adelsberger for the confocal laser scanning microscopy. We also thank Mrs. S. Kampf for expert technical assistance. This work was supported by the Deutsche Forschungsgemeinschaft SFB391 and Fonds der Chemischen Industrie.

References

[1] Hofmann, F., Lacinova, L. and Klugbauer, N. (1999) Rev. Physiol. Biochem. Pharmacol. 139, 33–86.
[2] Bosse, E., Regulla, S., Biel, M., Ruth, P., Meyer, H.E., Flockerzi, V. and Hofmann, F. (1990) FEBS Lett. 267, 153–156.
[3] Jay, S.D., Ellis, S.B., McCue, A.F., Williams, M.E., Vedvick, T.S., Harpold, M.M. and Campbell, K.P. (1990) Science 248, 490–492.
[4] Powers, P.A., Shuying, L., Hogan, K. and Gregg, R.G. (1993) J. Biol. Chem. 268, 9275–9279.
[5] Wissenbach, U., Bosse-Doenecke, E., Freise, D., Ludwig, A., Murakami, M., Hofmann, F. and Flockerzi, V. (1998) Biol. Chem. 379, 45–50.
[6] Iles, D.E., Segers, B., Weghuis, D.O., Suikerbuijk, R. and Wieringa, B. (1993) Cytogenet. Cell Genet. 64, 227–230.
[7] Singer, D., Biel, M., Lotan, I., Flockerzi, V., Hofmann, F. and Dascal, N. (1991) Science 253, 1553–1557.
[8] Wei, X., Perez-Reyes, E., Lacerda, A.E., Schuster, G., Brown, A.M. and Birnbaumer, L. (1991) J. Biol. Chem. 266, 21943–21947.
[9] Eberst, R., Dai, S., Klugbauer, S. and Hofmann, F. (1997) Pflug. Arch. 433, 633–637.
[10] Suh-Kim, H., Wei, X., Klos, A., Pan, S., Ruth, P., Flockerzi, V., Hofmann, F., Perez-Reyes, E. and Birnbaumer, L. (1996) Recept. Channels 4, 217–225.
[11] Letts, V.A., Felix, R., Biddlecome, G.H., Arikkath, J., Mahaffey, C.L., Valenzuela, A., Bartlett, F.S., Mori, Y., Campbell, K.P. and Frankel, W.N. (1998) Nat. Genet. 19, 340–347.
[12] Perez-Reyes, E., Cribbs, L.L., Daud, A., Lacerda, A.E., Barclay, J., Williamson, M.P., Fox, M., Rees, M. and Lee, J.-H. (1998) Nature 391, 896–899.
[13] Cribbs, L.L., Lee, J.-H., Yang, J., Satin, J., Zhang, Y., Daud, A., Barclay, J., Williamson, M.P., Fox, M., Rees, M. and Perez-Reyes, E. (1998) Circ. Res. 83, 103–109.
[14] Lee, J.-H., Daud, A.N., Cribbs, L.L., Lacerda, A.E., Pereverzev, A., Klöckner, U., Schneider, T. and Perez-Reyes, E. (1999) J. Neurosci. 19, 1912–1921.
[15] Klugbauer, N., Marais, E., Lacinova, L. and Hofmann, F. (1999) Pflug. Arch. 437, 710–715.
[16] Lacinova, L., Klugbauer, N. and Hofmann, F. (1999) J. Physiol. 516, 639–645.
[17] Dolphin, A.C., Wyatt, C.N., Richards, J., Beattie, R.E., Craig, P., Lee, J.-H., Cribbs, L.L., Volsen, S.G. and Perez-Reyes, E. (1999) J. Physiol. 519, 35–45.
[18] Black, J.L. and Lennon, V.A. (1999) Mayo Clin. Proc. 74, 357–361.
[19] Klugbauer, N., Lacinová, L., Marais, E., Hobom, M. and Hofmann, F. (1999) J. Neurosci. 19, 684–691.
[20] Ludwig, A., Flockerzi, V. and Hofmann, F. (1997) J. Neurosci. 17, 1339–1349.
[21] Hullin, R., Singer-Lahat, D., Freichel, M., Biel, M., Dascal, N., Hofmann, F. and Flockerzi, V. (1992) EMBO J. 11, 885–890.
[22] Perez-Reyes, E., Castellano, A., Kim, H.S., Bertrand, P., Baggstrom, E., Lacerda, A.E., Wei, X.Y. and Birnbaumer, L. (1992) J. Biol. Chem. 267, 1792–1797.
[23] Lambert, R.C., Maulet, Y., Mouton, J., Beattie, R., Volsen, S., DeWaard, M. and Feltz, A. (1997) J. Neurosci. 17, 6621–6628.
[24] Bourinet, E., Soong, T.W., Sutton, K., Slaymaker, S., Mathews, E., Monteil, A., Zamponi, G.W., Nargeot, J. and Snutch, T.P. (1999) Nat. Neurosci. 2, 407–415.
[25] Soong, T.W., Stea, A., Hodson, C.D., Dubel, S.J., Vincent, S.R. and Snutch, T.P. Structure and functional expression of a member of the low voltage-activated calcium channel family, (1993) Science 260, 1133–1136.
[26] Hobom, M., Marais, E., Lacinova, L., Klugbauer, N. and Hofmann, F. Identification of a new auxiliary calcium channel subunit expressed in human heart, (1999) Naunyn-Schmiedeberg's Arch. Pharmacol. 359, R67.